

A FINITE ELEMENT AND EXPERIMENTAL STUDY ON NOVEL 2D CHIRAL METAMATERIALS

LUKE MIZZI^{†*}, ARRIGO SIMONETTI[†], ANDREA SPAGGIARI[†]

[†]Department of Engineering Sciences and Methods (DISMI)
University of Modena and Reggio Emilia
Reggio Emilia, Italy

*e-mail: luke.mizzi@unimore.it

Key words: Auxetic Metamaterials, Chiral Honeycombs, Finite Element Analysis, Additive Manufacturing

Abstract.

Chiral honeycombs are a class of mechanical metamaterials which exhibit auxetic behaviour. As their name implies, these systems are characterised by ‘chirality’, i.e., they do not possess an axis/plane of mirror symmetry, and they deform primarily through node rotations and flexural deformation of ligaments. In this work, we used a combination of Finite Element simulations and experimental tests to analyse the mechanical properties, deformation behaviour and strain tolerance of a new class of chiral metamaterials based on 2D Euclidean polygonal tessellations. Numerical simulations on a range of periodic and finite systems were conducted in order to investigate the influence of geometric parameters on the Poisson’s ratio and effective Young’s modulus of these chiral honeycombs, while experimental compressive loading tests on 3D-printed prototypes were used to analyse their high-strain behaviour. The results obtained show that these systems, which exhibit transverse isotropy, have the ability to exhibit a wide spectrum of Poisson’s ratios ranging from high positive to large negative values as well as significant variation in stiffness which may be controlled as a function of a few key geometric parameters. These findings provide valuable insights on the functionality of these metamaterials and mark these systems as excellent candidates to be used as lightweight, high-porosity materials for potential future implementation in biomedical and aerospace applications.

1. INTRODUCTION

Auxetic metamaterials are a class of man-made materials which exhibit a negative Poisson's ratio. This unusual property is derived from their structure rather than chemical composition and, thus, auxeticity is scale-independent. In fact, this property has been observed at various scales, ranging from macroscopic additively-manufactured systems to thermo-/chemo-mechanically converted microscale foams, all the way to naturally occurring nanoscale crystals. There are various deformation modes and mechanisms which give rise to auxetic behaviour, with the most well-known being re-entrant honeycombs^[1], rotating unit modes^{[2],[3]}, chiral systems^{[4],[5]} and origami/folding patterns^[6]. Negative Poisson's ratio materials are also characterised by a number of additional unusual and useful properties which are directly derived from auxeticity. These include large indentation resistance and energy absorption properties, the ability to undergo synclastic (dome-shaped curvature) and superior acoustic and photonic properties with respect to conventional non-auxetic materials^{[7]–[11]}. These properties make these systems particularly well-suited for utilisation in niche applications in the fields of biomedical and aerospace engineering.

Due to their great potential, the design and development of novel auxetic metamaterials with advanced functionalities is an important step towards the future implementation of these materials in commonly-used everyday products. To this end, in this work we have designed and experimentally tested four novel chiral metamaterial systems which possess hexagonal rotational symmetry and exhibit transversely-isotropic mechanical properties. Chiral honeycombs are a class of auxetic structures which are characterised by 'chirality', i.e. an absence of axial symmetry, which means that the geometry of these systems is partially defined by their 'handedness'. The first chiral system proposed in the literature was the hexachiral honeycomb^{[4],[5]}. This metamaterial is defined by a circular chiral node connected by six tangentially-attached ligaments to adjacent identical nodes (see Figure 1a) and deforms primarily through rotation of nodes and flexure of ligaments. It is characterised by a Poisson's ratio of -1. Since the design of this system, various other chiral systems have been proposed, including the trichiral and tetrachiral honeycombs, as well as hierarchical and 3D systems (see Figure 1)^{[12]–[16]}. In addition, a class of related structures known as anti-chiral and meta-chiral metamaterials (which exhibit a certain degree of axial symmetry) with the ability to exhibit auxetic behaviour have also been proposed.

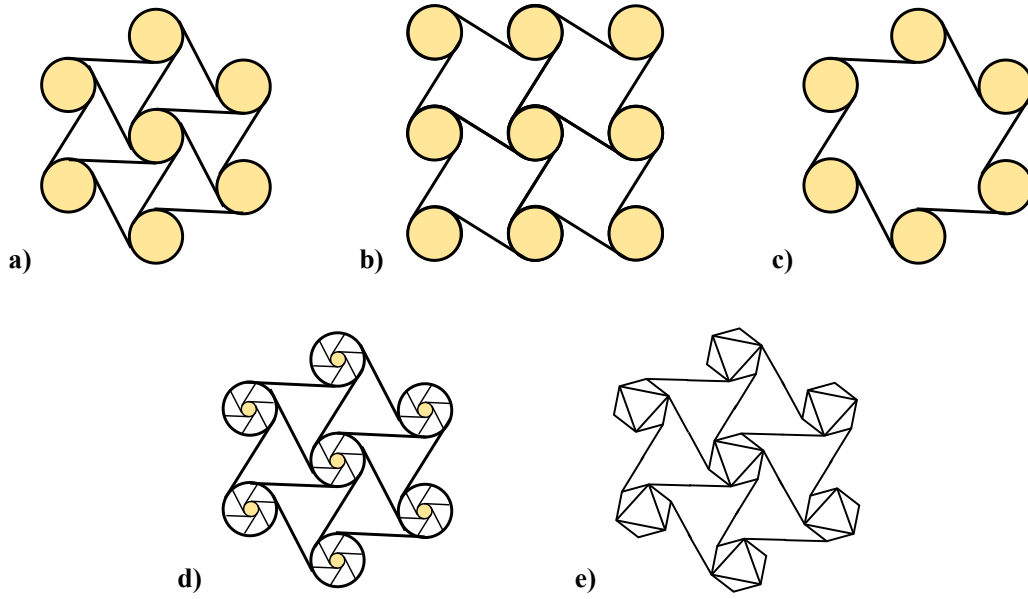


Figure 1: a) Hexachiral honeycomb, b) Tetrachiral honeycomb, c) Trichiral honeycomb, d) fractal hexachiral system and e) truss-based hierarchical hexachiral honeycomb.

Recently, we have proposed a novel class of chiral metamaterials based on Euclidean multi-polygonal tessellations and their dual counterparts^{[17],[18]}. These new metamaterials are designed through the ‘chiralisation’ of periodic tessellations, i.e. by placing chiral nodes at the vertices of the tessellations and connecting them through ligaments which bisect the sides of the original polygons. In this work, we present the results of a Finite Element analysis on the high strain compressive performance of four such metamaterial structures. The systems were simulated both as finite and periodic systems and subjected to large compressive strains. Furthermore, 3D-printed prototypes corresponding to the simulated systems were produced in ABS using an FDM Stratasys® 3D-printer and tested using a tensile loading machine in order to validate the numerical findings. The failure modes and collapse patterns of these chiral metamaterials were also observed and analysed, with the results obtained demonstrating extremely anomalous behaviours which are rare even in the field of auxetic metamaterials.

2. METHODOLOGY

As shown in Figure 2, the chiral systems investigated in this work were designed through the ‘chiralisation’ of two multi-polygonal tessellations exhibiting rotational symmetry of order 6 and their dual counterparts. The dual tessellations are derived directly from the original base tessellations through the formation of vertices at the centre points of the polygons which are connected together through lines bisecting the sides of the original tessellation^[19]. This means that the resultant dual systems retain the symmetry characteristics of the original tessellations.

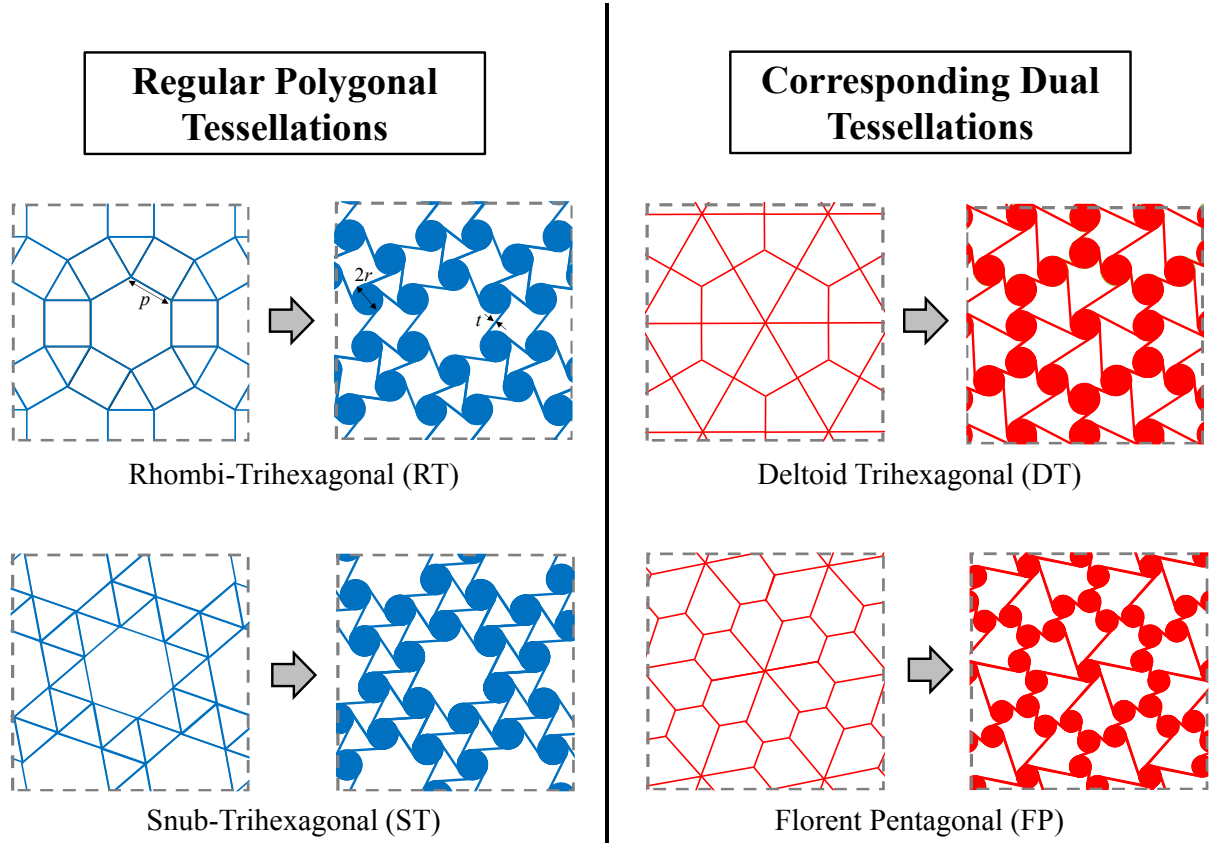


Figure 2: Diagram showing the base tessellations and chiralized equivalents investigated in this study.

The four tessellations studied in this work are denoted according to Conway's nomenclature^[20] as Rhombi-Trihexagonal (RT) with its corresponding dual tessellation being the Deltoid-Trihexagonal (DT) and Snub-Trihexagonal (ST) with its Florent Pentagonal (FP) dual equivalent. The chiral systems based on these tessellations are designed according to the following independent geometric parameters: the radius of the chiral node, r , the thickness of the ligament, t , and the side length of the original tessellation, p .

Finite Element simulations were used to analyse the behaviour of a sample set of these structures. The geometric parameters used, which were chosen on the basis of a previous parametric study^[17] on the linear mechanical properties of these systems, are listed in Table 1. The parameters were chosen with the specific aim of obtaining systems possessing Poisson's ratios with positive, negative and *quasi-zero* values whilst adhering to the resolution and platform size limits of the 3D printer at our disposal. The simulations were conducted under plane-stress conditions using the linear material properties of ABS ($E = 1000$ MPa and $\nu = 0.3$). The systems were subjected to uniaxial compressive strains. For each structure, a simulation was conducted utilizing periodic boundary conditions^[21] on a single representative unit cell as well as a second simulation on a finite 3×5 lattice structure with finite boundary conditions analogous to a standard experimental compressive loading test. The Poisson's ratio was then measured from the central unit cell of the system.

Table 1: Geometric parameters of the four chiralised tessellations studied

System	p (mm)	r (mm)	t (mm)
RT	15	4.5	0.9
DT	15	4.5	0.9
ST	15	3.7	0.9
FP	15	3.7	0.9

Experimental tests were also conducted on geometries analogous to the finite system simulations 3D-printed in ABS (see Figure 3). The prototypes were subjected to a mono-axial compressive loading test using a loading machine with a loadcell of 2500N. The force-displacement curve was obtained for each structure up to fracture in order to observe the failure modes of these chiral metamaterials. The Poisson's ratio of the systems was measured from the central representative unit cell for each using Digital Image Correlation (DIC) for small strains and the results were compared with the Finite Element results.

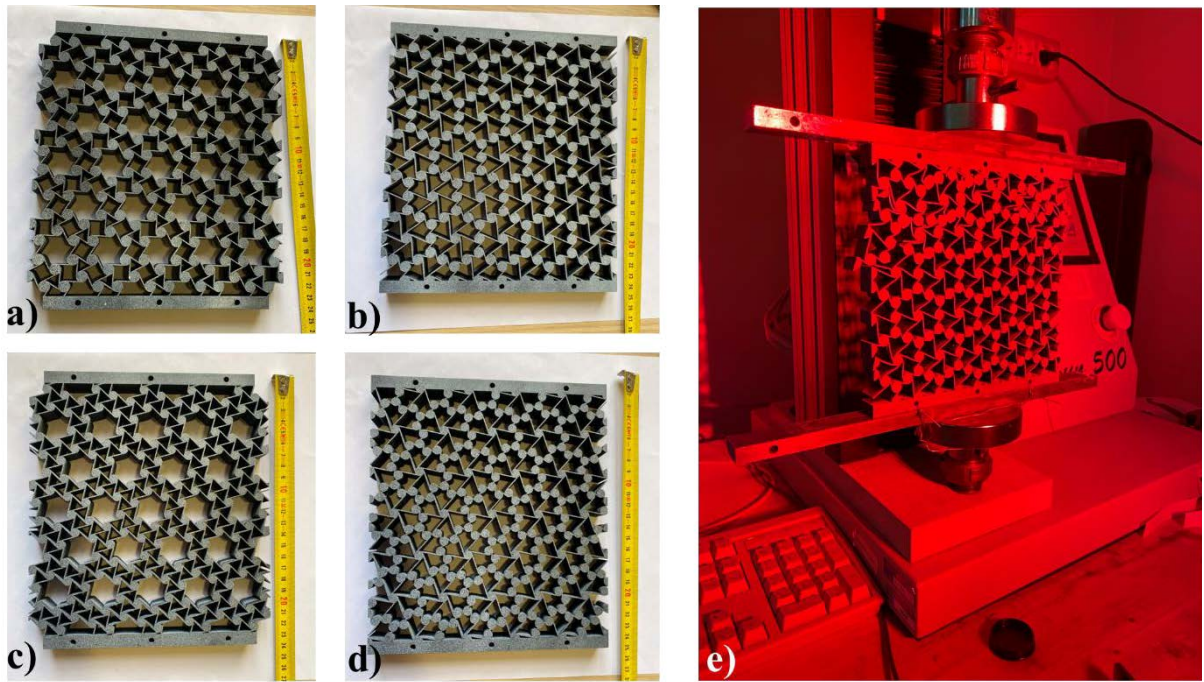


Figure 3: Experimental chiralized prototypes: a) RT, b) DT, c) ST and d) FP. Image e) shows a prototype mounted on the tensile loading machine under LED light for the DIC analysis.

3. RESULTS AND DISCUSSION

Table 2 shows the engineering Poisson's ratio obtained from the numerical simulations and the DIC measurements of the experimental test samples, while the force-displacement plots obtained from the experimental results are presented in Figure 4a. The experimental and FEM results show good agreement indicating that these chiral systems have the potential to exhibit both positive Poisson's ratios and auxetic behaviour. There similarity in the values obtained from the periodic simulations and finite simulations/experimental results also indicates that the influence of edge effects is minimal on the deformation behaviour of the central unit cell. The force-displacement plots also clearly demonstrate that system FP shows the highest level of structural stiffness while system RT is the weakest.

Table 2: Poisson's ratios obtained from the periodic and bounded Finite Element simulations and the experimental tests on the 3D-printed prototypes

System	Periodic Simulation ν	Finite Simulation ν	Experimental ν
RT	+0.314	+0.260	+0.283
DT	-0.322	-0.285	-0.246
ST	+0.039	+0.058	+0.148
FP	-0.487	-0.352	-0.318

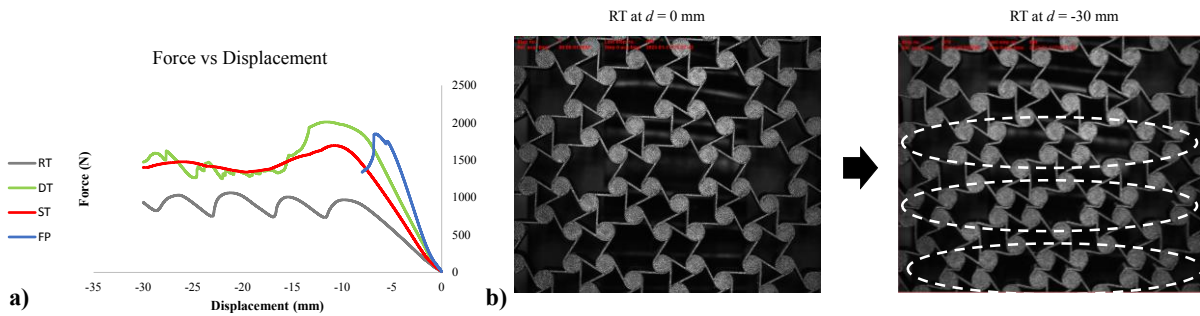


Figure 4: a) Force-displacement plots of the four prototypes up to fracture. In the case of FP, the system failed at a displacement value of -8 mm, while for the other systems the test was conducted up to -30 mm. b) Image showing the layer by layer sequential collapse of the system RT.

It is evident from Figure 4a) that the dual tessellations DT and FP have the highest level of structural stiffness. These systems are monohedral tessellations, i.e. their pores are all characterised by a single polygon (a quadrilateral for DT and a pentagon for FP), while the others tessellations are polyhedral (hexagons, squares and triangles for RT and hexagons and triangles for ST). This factor probably accounts for the fact that while the dual structures exhibited typical uniform failure modes for metamaterials starting from the borders subjected to compression (the upper and lower edges) and propagating through adjacent ligaments towards the centre, the multi-polygonal tessellations showed a more remarkable and unusual behaviour. In fact, in the latter systems, a sequential layer-by-layer collapse was observed which, however, did not propagate directly from one adjacent ligament to the next, but instead

was confined to a specific set of ligaments from each representative unit cell of the structure as shown in Figure 4b. This atypical behaviour is also evident from the force-displacement plots, particularly for RT, where the four sequential stepwise troughs and rises (see Figure 4a) represent the ordered collapse of four layers of vertically-aligned hexagonal pore ligaments (see Figure 4b).

4. CONCLUSIONS

In this work, we used FEM simulations and experimental tests on additively-manufactured prototypes to analyse the linear mechanical properties, deformation behaviour and high-strain failure modes of a new class of chiral metamaterials based on 2D Euclidean multi-polygonal tessellations. The results obtained showed that these systems, which are transversely-isotropic due to their rotational hexagonal symmetry, have the ability to exhibit positive, negative and *quasi-zero* Poisson's ratios as well as a wide variety of stiffness values. In addition, the high-strain analysis of these chiral systems revealed atypical, but ordered, fracture propagation patterns which could potentially be useful for the future design of metamaterial topologies with controlled failure modes.

References

- [1] I. G. Masters and K. E. Evans, "Models for the elastic deformation of honeycombs," *Compos. Struct.*, vol. 35, pp. 403–422, 1996.
- [2] J. N. Grima and K. E. Evans, "Auxetic behavior from rotating squares," *J. Mater. Sci. Lett.*, vol. 19, pp. 1563–1565, 2000.
- [3] J. N. Grima and K. E. Evans, "Auxetic behavior from rotating triangles," *J. Mater. Sci.*, vol. 1, pp. 3193–3196, 2006.
- [4] K. W. Wojciechowski and A. C. Branka, "Negative Poisson ratio in a two-dimensional "isotropic" solid," *Phys. Rev. A*, vol. 40, no. 12, pp. 7222–7225, 1989.
- [5] D. Prall and R. S. Lakes, "Properties of a chiral honeycomb with a Poisson's ratio of -1," *Int. J. Mech. Sci.*, vol. 39, no. 3, pp. 305–314, 1997.
- [6] M. Schenk and S. D. Guest, "Geometry of Miura-folded metamaterials," *Proc. Natl. Acad. Sci.*, vol. 110, no. 9, pp. 3276–3281, 2013.
- [7] L. Mizzi, E. Salvati, A. Spaggiari, J. Tan, and A. M. Korsunsky, "Highly stretchable two-dimensional auxetic metamaterial sheets fabricated via direct-laser cutting," *Int. J. Mech. Sci.*, vol. 167, no. October 2019, p. 105242, 2020.
- [8] F. Scarpa, J. Giacomini, Y. Zhang, and P. Pastorino, "Mechanical performance of auxetic polyurethane foam for antivibration glove applications," *Cell. Polym.*, vol. 24, no. 5, pp. 253–268, 2005.
- [9] J. Valente, E. Plum, I. J. Youngs, and N. I. Zheludev, "Nano- and Micro-Auxetic Plasmonic Materials," *Adv. Mater.*, pp. 5176–5180, 2016.
- [10] L. Mizzi, E. Salvati, A. Spaggiari, J. Tan, and A. M. Korsunsky, "2D auxetic metamaterials with tuneable micro-/nanoscale apertures," *Appl. Mater. Today*, vol. 20,

- p. 100780, 2020.
- [11] H. Lu, X. Wang, and T. Chen, “In-plane dynamics crushing of a combined auxetic honeycomb with negative Poisson’s ratio and enhanced energy absorption,” *Thin-Walled Struct.*, vol. 160, no. September 2020, p. 107366, 2021.
 - [12] A. Alderson *et al.*, “Elastic constants of 3-, 4- and 6-connected chiral and anti-chiral honeycombs subject to uniaxial in-plane loading,” *Compos. Sci. Technol.*, vol. 70, no. 7, pp. 1042–1048, 2010.
 - [13] A. Lorato *et al.*, “The transverse elastic properties of chiral honeycombs,” *Compos. Sci. Technol.*, vol. 70, no. 7, pp. 1057–1063, 2010.
 - [14] L. Mizzi *et al.*, “Mechanical metamaterials with star-shaped pores exhibiting negative and zero Poisson’s ratio,” *Mater. Des.*, vol. 146, pp. 28–37, 2018.
 - [15] Y. Zhu, Z. Zeng, Z. Wang, L. H. Poh, and Y. Shao, “Hierarchical hexachiral auxetics for large elasto- plastic deformation,” *Mater. Res. Express*, vol. 6, p. 085701, 2019.
 - [16] L. Mizzi and A. Spaggiari, “Lightweight mechanical metamaterials designed using hierarchical truss elements,” *Smart Mater. Struct.*, vol. 29, p. 105036, 2020.
 - [17] L. Mizzi and A. Spaggiari, “Chiralisation of Euclidean polygonal tessellations for the design of new auxetic metamaterials,” *Mech. Mater.*, vol. 153, p. 103698, 2021.
 - [18] L. Mizzi and A. Spaggiari, “Novel chiral honeycombs based on octahedral and dodecahedral Euclidean polygonal tessellations,” *Int. J. Solids Struct.*, vol. 238, p. 111428, 2022.
 - [19] B. Grünbaum and G. C. Shephard, *Tillings and Patterns*, 2nd ed. Dover Publications, 2016.
 - [20] J. H. Conway, H. Burgiel, and C. Goodman-Strauss, “Archimedean Tilings,” in *The Symmetry of Things*, A. K. Peters, Ed. CRC Press, 2008.
 - [21] L. Mizzi, D. Attard, R. Gatt, K. K. Dudek, B. Ellul, and J. N. Grima, “Implementation of periodic boundary conditions for loading of mechanical metamaterials and other complex geometric microstructures using finite element analysis,” *Eng. Comput.*, vol. 37, no. 3, pp. 1765–1779, 2021.